Na₂Ga₇

NaLiGa₇

Li₂B₁₂Si₂

MgB₁₂Si₂

Showcasing research at the Department of Chemical Metals Science at the Max Plank Institute for Chemical Physics of Solids in Dresden.

Ordering by cation replacement in the system $Na_{2-x}Li_xGa_7$

$Na_1Li_1Ga_7$ represents a new variant within the $MgB_{12}Si_2$ structure family. The arrangement of cations is fully ordered. Considering a framework of *closo* Wade clusters $[(12b)Ga_{12}]^{2-}$ and Zintl anions $[(4b)Ga]^-$ the compound can be classified as a Zintl–Wade phase.
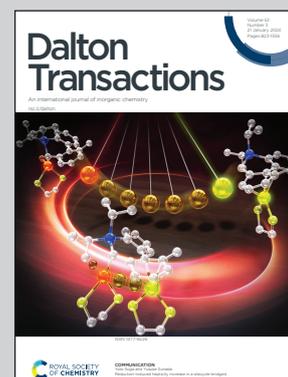
ROYAL SOCIETY OF CHEMISTRY

Check for updates

Ordering by cation replacement in the system Na₂₋ₓLiₓGa₇†

Chia-Chi Yu,[a] Yurii Prots,[a] Alim Ormeci,[a] Mitja Krnel, [iD][a] Marcus Schmidt,[a] Lev Akselrud,[a,b] Frank R. Wagner, [iD][a] Yuri Grin[a] and Michael Baitinger [iD] *[a]

Samples of the pseudo-binary system $Na_{2-x}Li_xGa_7$ ($x \leq 1$) were synthesized from the elements at 300 °C in sealed Ta ampoules or by the reaction of Na_2Ga_7 with LiCl. The peritectic formation temperature decreases with increasing Li content from 501(2) °C ($x = 0$) to 489(2) °C ($x = 1$). The boundary compositions Na_2Ga_7 and $Na_1Li_1Ga_7$ crystallize with different structure types related by a group–subgroup relation. While the Na-rich compositions ($x \leq 0.5$) represent a substitutional solid solution (space group *Pnma*), the Li-rich compositions feature an unconventional replacement mechanism in which Li atoms occupying interstitial positions induce vacancies at the Na positions (space group *Cmce*). The crystal structure of $Na_1Li_1Ga_7$ ($a = 8.562(1)$ Å, $b = 14.822(2)$ Å, $c = 11.454(2)$ Å; $Z = 8$) was determined from X-ray single-crystal diffraction data, and reveals an anionic framework comprising 12-bonded Ga_{12} icosahedra and 4-bonded Ga atoms, with alkali–metal atoms occupying channels and cavities. The arrangement of cations makes $NaLiGa_7$ a new structure type within the $MgB_{12}Si_2$ structure family. Band structure calculations for the composition $NaLiGa_7$ predict semiconducting behavior consistent with the balance $[Na^+]_2[Li^+]_2[(Ga_{12})^{2-}][Ga^-]_2$, considering *closo* Wade clusters $[(12b)Ga_{12}]^{2-}$ and Zintl anions $[(4b)Ga]^-$. Susceptibility measurements indicate temperature-independent diamagnetic behavior.

Introduction

Inorganic framework compounds composed of p-elements and encapsulated metal cations are frequently studied.[1,2] Their crystal structures show the characteristic bonding features of the framework atoms involved. While clathrate-type structures are commonly observed among frameworks based on 4-bonded group 14 elements,[1] frameworks of group 13 elements lack valence electrons to solely form two-center, two-electron bonds between all framework atoms.[2] They typically adopt polyhedral Wade clusters, such as *closo* $[B_6]^{2-}$ in CaB_6,[3] or form multiatomic bonds, like in $BaAl_4$,[4] which may be considered as a framework of 2D edge-condensed *nido* clusters. An example of the first type is the recently discovered Na_2Ga_7,[5] which exhibits a framework of 12-bonded $[Ga_{12}]^{2-}$ *closo* clusters and 4-bonded $[Ga]^-$ Zintl anions. The electronic balance is achieved by the Na cations according to $[Na^+]_4[(Ga_{12})^{2-}][Ga^-]_2$. The structure of this family can also be formed with heteroatomic frameworks and varying cation contents, as evidenced by the boride silicides $MgB_{12}Si_2$[6] and $Li_2B_{12}Si_2$,[7] which are composed of $[B_{12}]^{2-}$ *closo* clusters and 4-bonded Si atoms. In contrast to the boride silicides, the higher number of cations in Na_2Ga_7 (*i.e.* $Na_4Ga_{12}Ga_2$) leads to their disorder in the Ga channels. In this study, we investigate the pseudo-binary system $Na_2Ga_7/NaLiGa_7$ to determine the response of the Ga framework on the cation substitution and the possibility to obtain new members of the $MgB_{12}Si_2$ family.

Experimental details

Preparation

Reaction from the elements. Na (Chempur, 99.9%), Li (EVOCHEM, 99.9%) and Ga (Chempur, 5 N) were combined in a total amount of 2 g to prepare the compositions $Na_{2-x}Li_xGa_7$ ($x = 0.2, 0.5, 0.8, 1.0, 1.5$) and, with excess of Li, $Na_1Li_{1.2}Ga_7$. The mixtures were sealed in Ta tubes under an Ar atmosphere. For homogenization, the sample was heated to 1000 °C for 2 min using an induction furnace and then allowed to cool to room temperature by turning off the furnace. Subsequently, the Ta tube was placed in a quartz vessel and further annealed under vacuum at 300 °C for one week. After annealing, the ampoule was quenched in water. The reaction products consisted of crystalline grains with metallic luster and were sensitive to air and moisture.

[a]*Max-Planck-Institut für Chemische Physik fester Stoffe, Nöthnitzer Str. 40, 01187 Dresden, Germany. E-mail: Michael.Baitinger@cpfs.mpg.de*
[b]*Ivan Franko Lviv National University, Kyryla i Mefodia St. 6, 29005 Lviv, Ukraine*
†Electronic supplementary information (ESI) available. CCDC 2304096 (NaLiGa₇). For ESI and crystallographic data in CIF or other electronic format see DOI: https://doi.org/10.1039/d3dt03628f

Metathesis reaction. Finely ground powder mixtures of Na_2Ga_7 [5] and LiCl (Chempur, 99.9%) were mixed with molar ratios of 1 : 1 or 1 : 1.5. These mixtures were pressed into pellets (d = 10 mm, h = 2 mm), sealed in a Ta crucible under an Ar atmosphere, and placed in an evacuated glass vessel. The vessel was annealed at 300 °C in a tube furnace for one week and then cooled down to room temperature by switching off the furnace.

Characterization

Single-crystal X-ray diffraction. A single crystal of $NaLiGa_7$ was fixed on top of a glass capillary (d = 0.1 mm) with grease and sealed in another capillary (d = 0.3 mm). Room-temperature single-crystal X-ray diffraction data were collected by a Rigaku AFC7 diffractometer (Saturn 724+ CCD detector, Mo Kα radiation, λ = 0.71073 Å). Absorption correction was performed with a multi-scan procedure. The crystal structure was solved and refined by using the WinCSD program.[8] Details about the data collection and structure refinement are listed in Table S1;† atomic coordinates and displacement parameters are shown in Table S2;† selected interatomic distances and angles are listed in Tables S3–5.† The program Diamond V4.6.8 was used for structure drawings.[9]

Powder X-ray diffraction (PXRD). All samples were characterized by the Guinier technique (Huber Image Plate Camera G670; germanium monochromator; Cu Kα1 radiation; λ = 1.54056 Å; 5.0° < 2θ < 100°; step width = 0.005°). Finely ground specimens were fixed under an Ar atmosphere on the sample holder between two polyimide foils (7.5 μm, Kapton, Chemplex), using a thin film of vacuum grease (Lithelen, Leybold). LaB_6 standard (NIST, SRM 660a) was added to the sample as a reference for the reflection positions. Lattice parameters were obtained from the least-square method, using reflection positions extracted by profile fitting.[8]

Scanning electron microscope (SEM). Compositional analysis by EDX failed as polishing of the air- and moisture-sensitive material always led to the formation of a gallium layer on the sample surface.

Thermal analysis. The thermal behaviour of the samples $Na_{2-x}Li_xGa_7$ was measured with a heat-flux DTA device (Netzsch DSC 404C). About 50 mg of a pure sample was sealed in a Nb crucible (d = 5 mm, 600 mg). The system was heated from room temperature up to 600 °C then cooled down to 100 °C with heating rate of 5 °C min^{-1} under an Ar atmosphere. The measurements were calibrated with elemental Al measured under the same conditions. For thermal decomposition analysis, 50 mg of finely ground powder of $NaLiGa_7$ was filled under an Ar atmosphere in an open Ta crucible. For the heat treatment, the Ta crucible was placed in a glass tube, which was evacuated to 10^{-2} mbar and closed. During the heat treatment, the decomposition is evidenced by the precipitation of a sodium mirror at the cold part of the glass vessel. After the measurement, the product was characterized by PXRD.

Magnetic susceptibility. Magnetization was measured in a SQUID magnetometer (MPMS-XL7, Quantum Design) in the temperature range 1.8–400 K. Fields μ_0H from 2 mT to 7 T

were applied, the diamagnetic contribution of the sample tube was subtracted.

Calculation methods. First-principles electronic structure calculations were conducted using the all-electron full-potential local orbital (FPLO) method.[10] Exchange–correlation effects were considered *via* the local density approximation (LDA) within the density functional theory, utilizing the Perdew and Wang parametrization.[11] The experimentally obtained crystal structure data were utilized. The Brillouin zone was sampled with a 15 × 15 × 15 mesh.

Results and discussion

Preparation of $Na_{2-x}Li_xGa_7$ ($x \leq 1$)

When a stoichiometric mixture of the elements at composition $NaLiGa_7$ was melted and cooled down to room temperature within a few minutes, the resulting product predominantly consisted of $NaLiGa_7$, along with smaller amounts of Li_3Ga_{14} [12] and an unidentified phase, as determined by PXRD analysis. This behaviour notably differs from the preparation of Na_2Ga_7, which does not form directly from the melt.[5] However, the presence of foreign phases indicates that $NaLiGa_7$ forms incongruently as well. Subsequent annealing at 300 °C for one week led to the formation of single-phase products for all compositions $Na_{2-x}Li_xGa_7$, with x = 0.2, 0.5, 0.8 and 1 as confirmed by PXRD analysis (Fig. 1). For the sample with x = 1.5, the majority phase was $Na_1Li_1Ga_7$, accompanied by foreign phases (Table 1). During annealing, the sample melted partially, indicating that the identified phases, $Na_1Li_1Ga_7$, Li_3Ga_{14}, $LiGa_2$ and $LiGa_6$,[13] were not in equilibrium upon cooling. Therefore, we conclude that the upper limit for
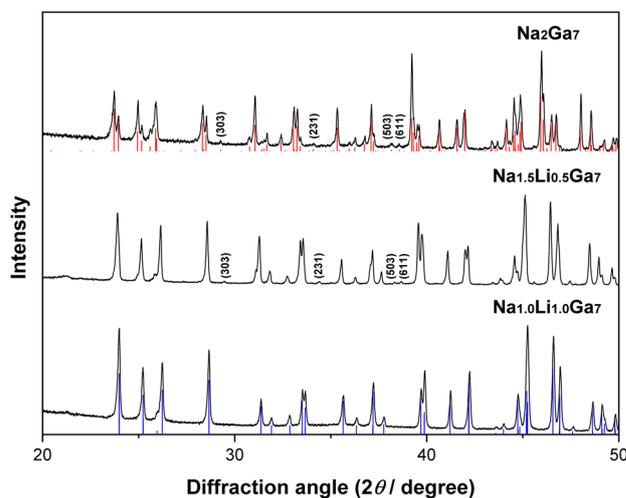
Fig. 1 PXRD patterns of $Na_{2-x}Li_xGa_7$ (x = 0, 0.5, 1) after annealing at 300 °C (Cu Kα1). The calculated patterns of Na_2Ga_7 (space group *Pnma*, red lines) and $NaLiGa_7$ (space group *Cmce*, blue lines) are based on single-crystal diffraction data. For $Na_{1.5}Li_{0.5}Ga_7$ and Na_2Ga_7, some characteristic reflections breaking the C-centered lattice are indexed. In $NaLiGa_7$, symmetry inequivalent reflections overlap due to the hexagonal axis ratio b/a (Table 1).

Table 1 Lattice parameters of samples with the nominal compositions $Na_{2-x}Li_xGa_7$ (x = 0, 0.2, 0.5, 0.8, 1, 1.5) and $NaLi_{1.2}Ga_7$ obtained by annealing at 300 °C. PXRD patterns of samples with $x \leq 0.5$ show primitive reflections breaking the $Cmce$ symmetry. For a better comparison of the lattice parameters, samples with x = 0, 0.2, and 0.5 are listed in the non-standard setting $Pmnb$ instead of $Pnma$

| Nominal composition | x | Lattice parameters | | | | Space group | b/a |
		a/Å	b/Å	c/Å	V/Å³		
Na_2Ga_7	0	8.6766(6)	14.8580(6)	11.6105(5)	1497.1(1)	$Pmnb$	1.7124(1)
$Na_{1.8}Li_{0.2}Ga_7$	0.2	8.646(2)	14.847(3)	11.558(3)	1483.7(6)	$Pmnb$	1.7172(5)
$Na_{1.5}Li_{0.5}Ga_7$	0.5	8.5956(9)	14.834(1)	11.488(2)	1464.8(3)	$Pmnb$	1.7257(2)
$Na_{1.2}Li_{0.8}Ga_7$	0.8	8.5692(9)	14.836(2)	11.466(2)	1457.7(4)	$Cmce$	1.7313(3)
$Na_{1.0}Li_{1.0}Ga_7$	1	8.562(1)	14.822(2)	11.454(2)	1453.6(4)	$Cmce$	1.7311(3)
$Na_{0.5}Li_{1.5}Ga_7$	1.5	8.584(7)	14.80(2)	11.444(6)	1453(4)	$Cmce$	1.724(3)
$Na_{1.0}Li_{1.2}Ga_7$	—	8.558(1)	14.820(2)	11.453(2)	1452.6(3)	$Cmce$	1.7317(3)

substitution of Na atoms is reached at x = 1. Furthermore, a homogeneity range $Na_1Li_{1+\delta}Ga_7$ with a higher Li content was not detected by refinement of the lattice parameters. The product with nominal composition $Na_1Li_{1.2}Ga_7$ consisted of $Na_1Li_1Ga_7$ and exhibited weak reflections of an unknown phase.

Other than from direct synthesis, $Na_1Li_1Ga_7$ can be formed through a metathesis reaction of Na_2Ga_7 and LiCl (eqn (1)). The reaction is supported by the higher stability of NaCl compared to LiCl increasing with temperature.[14] When Na_2Ga_7 and LiCl were reacted in a 1 : 1 molar ratio at 300 °C, the product consisted of $Na_1Li_1Ga_7$ and NaCl as confirmed by PXRD analysis (Table 2).

No residual LiCl was detected, and the refined lattice parameter of NaCl (a = 5.6400(7) Å) matched the reported value.[15] This indicates that the cation substitution was quantitative.

$$1\ Na_2Ga_7 + 1\ LiCl \rightarrow 1\ Na_1Li_1Ga_7 + 1\ NaCl \qquad (1)$$
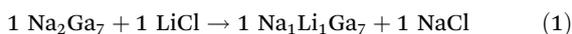
When Na_2Ga_7 was reacted with 1.5 equivalents of LiCl at 300 °C, a mixture of $Na_{2-x}Li_xGa_7$, Li_3Ga_{14} and NaCl was observed in PXRD. The overlapping reflections lowered the precision of the lattice parameter refinement, but the obtained values are consistent with the composition $NaLiGa_7$. This finding confirms that Li can substitute up to one equivalent of Na in Na_2Ga_7. With an excess amount of LiCl, $Na_1Li_1Ga_7$ was not formed. Reacting an equimolar mixture of $NaLiGa_7$ and LiCl resulted in the formation of binary gallides Li_3Ga_{14}, $LiGa_2$ and $NaGa_4$.[16]

Thermal stability of the composition range $Na_{2-x}Li_xGa_7$

The binary phase Na_2Ga_7 forms peritectically at 501(2) °C from Na_7Ga_{13}[17] and the melt.[5] Regarding the ternary system $Na_{2-x}Li_xGa_7$, the thermal stability decreases with increasing Li content. A single-phase sample of $Na_{1.8}Li_{0.2}Ga_7$ revealed a slightly lower decomposition temperature of T = 498(2) °C. At the maximum Li-content $Na_1Li_1Ga_7$, the formation temperature is further reduced to T = 489(2) °C. At all compositions of $Na_{2-x}Li_xGa_7$, the presence of two signals in the DTA experiments indicates that the samples undergo incongruent melting (Table S6†).

The thermal decomposition of $Na_1Li_1Ga_7$ was investigated on bulk material to examine the possibility of the formation of a new ternary phase through the evaporation of Na. However, no such phase was observed. Under static vacuum conditions at 300 °C, no reaction was observed, and the initial material remained unchanged for a period of 1 week. At 400 °C, after 1 day, sodium droplets were observed in the cooler region of the glass reactor. PXRD patterns of the solid residue consisted of $NaLiGa_7$, minor amounts of Li_3Ga_{14} and amorphous Ga, as indicated by its characteristic background. When the reaction time was prolonged to 3 days, only Li_3Ga_{14} was detected along with contributions of amorphous Ga (eqn (2)).

$$3\ Na_1Li_1Ga_7 \rightarrow 1\ Li_3Ga_{14} + 7\ Ga + 3\ Na \uparrow \qquad (2)$$
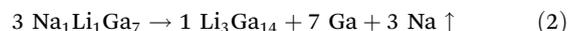
Crystal structure of $Na_{2-x}Li_xGa_7$

Structure determination. The crystal structure of $NaLiGa_7$ was determined using single-crystal XRD data, revealing an orthorhombic unit cell with the space group $Cmce$ (no. 64). The direct structure solution revealed five independent Ga positions, forming a framework consisting of icosahedral cluster units (Ga1–Ga4) and 4-bonded atoms (Ga5). A mixed occupancy of Ga and Li as it was recently detected in covalent Ge networks[18–20] was not observed. After refining the Ga posi-

Table 2 Lattice parameters of $NaLiGa_7$ obtained from different preparation methods. Parameters were refined from the same set of non-overlapping reflections

| Method | Lattice parameters | | | | Space group |
	a/Å	b/Å	c/Å	V/Å³	
Cast product	8.554(2)	14.826(3)	11.457(2)	1453.0(5)	$Cmce$
Annealing at 300 °C	8.562(1)	14.822(2)	11.454(2)	1453.6(4)	$Cmce$
1 Na_2Ga_7 + 1 LiCl	8.5622(9)	14.828(2)	11.458(2)	1454.7(4)	$Cmce$

tions, the cation positions were determined from the difference Fourier map. Two distinct peaks were identified, with the larger one located within the channels of the Ga framework, and a smaller peak situated in a cavity between three Ga_{12} icosahedra. Assigning the larger peak at Wyckoff position $8e$ to Na and the weaker one at Wyckoff position $8f$ to Li, subsequent refinement cycles were performed with an anisotropic approximation of the atomic displacement parameters (ADPs). These refinement cycles resulted in full occupancy for all positions and yielded a residual value of $R_F = 0.040$. The ADPs of all Ga atoms and Li exhibited nearly isotropic behavior with regular U_{eq} values. Only for the Na atom, the ADPs showed a distinct ellipsoidal shape with a larger U_{eq} value (Fig. S1†). The orientation of the Na ellipsoids aligns to the walls of the channels, which run in a zig-zag pattern along the [100] direction (Fig. S2†). The disorder can be modeled by splitting the Na1 position ($8e$) into a 0.5-occupied Na1a position ($8e$) and a 0.25-occupied Na1b position ($16g$). In the final refinement cycle, the restraint $occ(Na1a) + 2 \times occ(Na1b) = 1$ was applied, leading to a further reduction of the residual value R_F to 0.034. The refined unit-cell composition $Na_8Li_8Ga_{56}$ ($Na_1Li_1Ga_7$ with $Z = 8$) is electronically balanced according to $[Na^+]_8[Li^+]_8[(Ga_{12})^{2-}]_4[Ga^-]_8$, assuming the presence of *closo* Wade clusters[21,22] $[(12b)Ga_{12}]^{2-}$ and Zintl anions[23–25] $[(4b)Ga]^-$. Unlike $NaLiGa_7$, all other compounds in the series $Na_{2-x}Li_xGa_7$ with $x \leq 0.5$ crystallize with the subgroup *Pnma*. The lower symmetry is evident from the presence of additional reflections indexed in the PXRD patterns, *e.g.* (303), (231), (503) and (611), which violate the reflection conditions for space group *Cmce* (Fig. 1). Also, for another reason, the powder diffraction pattern of Na_2Ga_7 is more line-rich than that of $NaLiGa_7$. The lattice parameters a and b in $NaLiGa_7$ exhibit the almost ideal hexagonal ratio of $\sqrt{3}$, whereas in Na_2Ga_7, this value is not reached (Table 1). Therefore, reflections that overlap in $NaLiGa_7$, separate in Na_2Ga_7. The crystal structure of samples with compositions $Na_{2-x}Li_xGa_7$ ($x = 0.2, 0.5, 0.8$) was determined by the Rietveld method (Tables S7–S9†). In the initial structure model, the Ga positions were adopted from Na_2Ga_7[5] and refined with isotropic ADPs. Subsequently, the positions of cations were determined. The partial occupancy of Na and Li positions could only be approximated.

Structure description. Compounds of the $MgB_{12}Si_2$ family feature a characteristic framework composed of E13 elements, which can be partially replaced by E14 elements.[5–7] The framework is built up of a face-centered arrangement of icosahedra, bonded together by exohedral bonds and 4-bonded atoms (Fig. S3†). While the overall framework topology is characteristic for all representatives, the cation positions vary depending on number and size of the cations in relation to the framework. While the anionic framework can always be described with space group *Cmce*, the cation arrangement in turn can lower the space group symmetry. Among the known representatives, $MgB_{12}Si_2$ and Na_2Ga_7 crystallize in the space group *Pnma*, while $Li_2B_{12}Si_2$ and $Na_1Li_1Ga_7$ crystallize in the space group *Cmce* (Table 3). The framework offers three distinct cation positions (Fig. 2), which are located along channels

Table 3 Cation arrangement in compounds of the $MgB_{12}Si_2$ structure family. Three cation positions are available in the B/Si or Ga framework (M = Mg, Li, Na; F = B, Si, Ga)

| Compound | Occupancy (in %) | | | M/F | Space group |
	C1	C2	C3		
$MgB_{12}Si_2$	50	0	0	1 : 14	*Pnma*
$Li_2B_{12}Si_2$	100	0	0	2 : 14	*Cmce*
Na_2Ga_7	50	100	50	4 : 14	*Pnma*
$NaLiGa_7$	0	100	100	4 : 14	*Cmce*
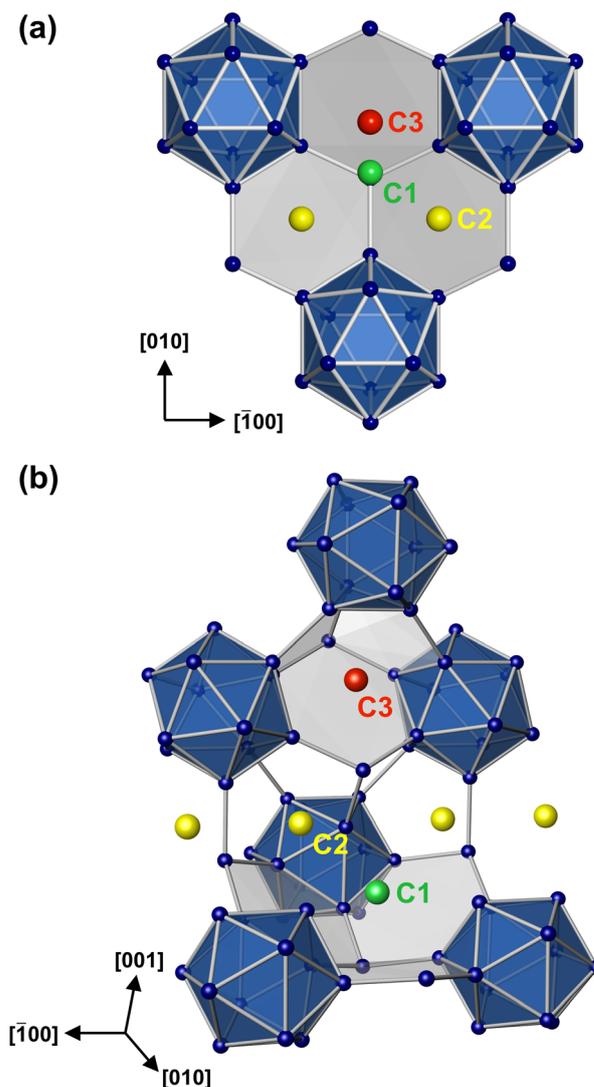
Fig. 2 (a) Local environment of the cation positions **C1**, **C2** and **C3** in $NaLiGa_7$. (b) Positions **C1** and **C3** are alternatively occupied.

oriented in the [100] direction in the *Cmce* setting and in the [010] direction in the *Pnma* setting (Fig. 3). The potential cation positions can be visualized on a plane obtained by sectioning the three-dimensional framework perpendicular to the [001] direction (Fig. 4). The most favorable cation position
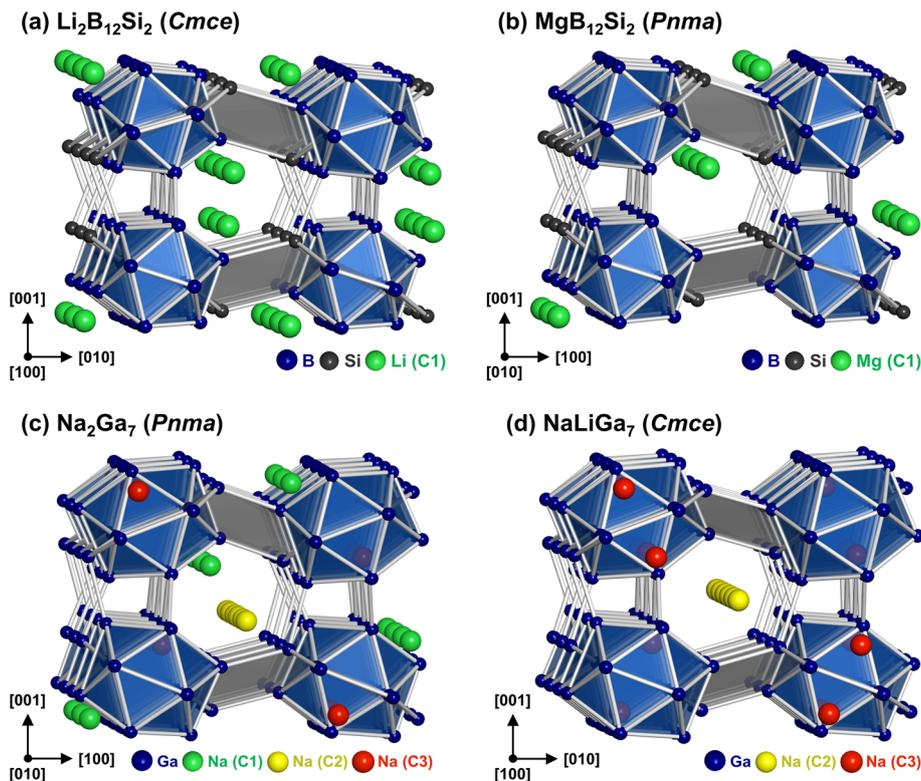
(a) Li$_2$B$_{12}$Si$_2$ (*Cmce*)

(b) MgB$_{12}$Si$_2$ (*Pnma*)

(c) Na$_2$Ga$_7$ (*Pnma*)

(d) NaLiGa$_7$ (*Cmce*)

Fig. 3 Cation positions for the representatives of the MgB$_{12}$Si$_2$ family: (a) Li$_2$B$_{12}$Si$_2$, (b) MgB$_{12}$Si$_2$, (c) Na$_2$Ga$_7$ and (d) NaLiGa$_7$.

seems to be the one denoted **C1**, which is located in the channels and the only occupied position in the compounds MgB$_{12}$Si$_2$ and Li$_2$B$_{12}$Si$_2$. At **C1**, the cations occupy hollows formed by three condensed six-membered rings (Fig. 2b).

In the boride silicide Li$_2$B$_{12}$Si$_2$, all **C1** positions are filled by Li atoms (Fig. 3a, 4a), while in MgB$_{12}$Si$_2$ only half of them are occupied by Mg atoms (Fig. 3b, 4b). The partial occupancy manifests in such a way that in each channel half positions are removed. In this way, the partial occupancy leads to a reduction in symmetry from *Cmce* in Li$_2$B$_{12}$Si$_2$ to *Pnma* in MgB$_{12}$Si$_2$. The crystal structure of Na$_2$Ga$_7$ (≡Na$_4$Ga$_{12}$Ga$_2$) contains twice as many cations as Li$_2$B$_{12}$Si$_2$, so that the occupation of all positions **C1** is not sufficient to accommodate all Na atoms. Consequently, two additional cation positions **C2** and **C3** are found, which have not been observed in the boride silicides (Fig. 3c, 4c). Atoms at position **C2** are also located in the channels (Fig. 2b), which creates a conflict with the spatial requirements of the atoms at **C1**. In Na$_2$Ga$_7$, full occupancy of **C1** and **C2** in the channels by Na atoms is impossible for steric reasons. The maximum filling of the channels is achieved, when 50% of the **C1** positions and 100% of **C2** are occupied. The replaced **C1** atoms occupy **C3** positions instead, located in small cavities between three Ga$_{12}$ icosahedra (Fig. 2b). However, only half of the available **C3** positions are occupied by Na atoms. Always two **C3** positions are arranged in close proximity (Fig. 5), resulting in a distance d(**C3**–**C3**) = 2.78 Å being too short if both neighboring positions were filled by Na. The half occupancy of **C1** and **C3** in Na$_2$Ga$_7$ along with the

ordered arrangement of Na results in a symmetry reduction from *Cmce* to *Pnma*.

In the crystal structure of NaLiGa$_7$, the smaller Li atoms fill up all **C3** positions. Simultaneous occupation of the adjacent positions **C1** and **C3** is excluded for their short distance of ≈1.60 Å requiring the **C1** positions to remain empty. The **C2** positions in the channels of NaLiGa$_7$ are fully occupied by Na atoms (Fig. 3d, 4d), as in Na$_2$Ga$_7$. With full occupancy of **C3**, there is no symmetry reduction observed in NaLiGa$_7$ and the space group remains *Cmce* (Table 3). The arrangement of cations in NaLiGa$_7$ introduces a new structure type within the MgB$_{12}$Si$_2$ structure family.

The topology of the Ga framework in NaLiGa$_7$ is very similar to the one in Na$_2$Ga$_7$. The Ga$_{12}$ icosahedra are distorted with endohedral bond distances ranging from 2.601(1) Å to 2.817(1) Å. The distances between atoms in *trans*-position vary from d(Ga3–Ga3) = 4.902 Å to d(Ga2–Ga2) = 5.338 Å (Fig. S4 and S5†). As expected, the exohedral two-center, two-electron bonds ($\bar{d}_{exo}$ = 2.54 Å) are shorter than the endohedral multicenter bonds ($\bar{d}_{endo}$ = 2.67 Å). The longest Ga–Ga bond d(Ga4–Ga4) = 2.817 Å is found at the cavity position **C3**, which shows that the occupation of this position creates distortion in the framework. For the boride silicides, where **C3** is not occupied, this distortion of the icosahedra does not occur. The 4-bonded atoms Ga5 deviate from ideal tetrahedral coordination with bond angles ranging from 97.59(1) to 123.83(4) degrees and bond distances ranging from 2.517 Å to 2.591 Å. Comparing the bond spectra of Na$_1$Li$_1$Ga$_7$ and Na$_2$Ga$_7$, the
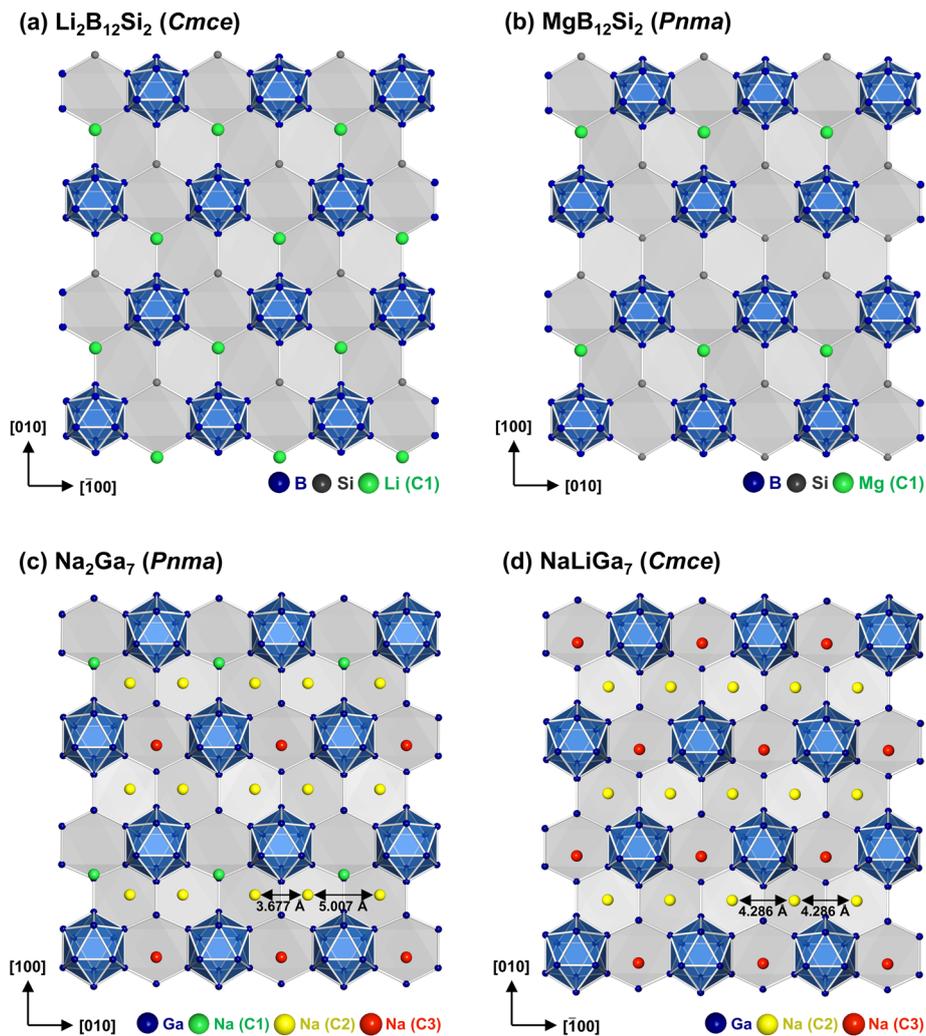
Fig. 4 Puckered hexagon layers of (a) $Li_2B_{12}Si_2$, (b) $MgB_{12}Si_2$, (c) Na_2Ga_7 and (d) $NaLiGa_7$. For $NaLiGa_7$, the mean position of the split sites Na1a/Na1b (**C2** position) is shown.
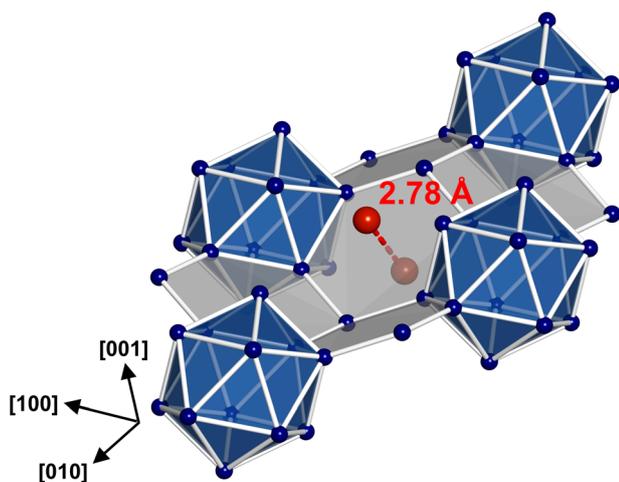

**Fig. 5** Pair of Li atoms situated in adjacent **C3** cavities having a distance of 2.78 Å.

framework in $Na_1Li_1Ga_7$ shows a smaller dispersion of the Ga–Ga bond lengths (Fig. 6). The dispersion of bond lengths in Na_2Ga_7 is mainly caused by the accommodation of the larger Na atoms in 50% of the small **C3** cavities. In agreement with the reduced cell volume, the mean Ga–Ga bond distance in $Na_1Li_1Ga_7$ of 2.62 Å is shorter than 2.66 Å in Na_2Ga_7.

Structural evolution in the composition range $Na_{2-x}Li_xGa_7$. When Na atoms are substituted with Li atoms, the unit-cell volume decreases with increasing Li content (Fig. 7a). However, for compositions with $x \leq 0.5$ (space group *Pnma*), the volume reduction is more pronounced than for compositions with $x > 0.5$ (space group *Cmce*). Hence, different substitution mechanisms are at work. This can be understood by considering the occupancies of the cation positions (Table S10†):

• In Na_2Ga_7, the positions **C1** and **C3** are half-occupied by Na.

• In $NaLiGa_7$, **C1** is empty, while **C3** is fully occupied by Li.

• In both phases, position **C2** is entirely filled with Na atoms
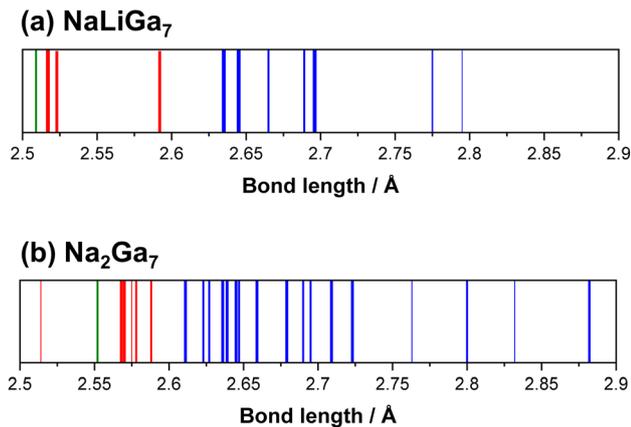
Fig. 6 Distance spectra in the Ga framework of (a) $NaLiGa_7$ and (b) Na_2Ga_7. Blue: endohedral bonds of the Ga_{12} icosahedra; green: exohedral bonds between icosahedra; red: exohedral bonds between the icosahedra and 4-bonded Ga atoms.

To determine the cation site occupancies for the compositions between $0 < x < 1$, only PXRD data were available (Table S11†). The accuracy of the derived structure models was further constrained by the low scattering power of Li located in proximity to the heavier Ga atoms. Despite of these experimental limitations, the substitution mechanism can be inferred: For $0 \leq x \leq 0.5$, the Na occupancy at **C1** remains constant, while the Na occupancy at **C3** clearly decreases (Fig. 7b).

Consequently, starting from Na_2Ga_7, the Li atoms first replace Na atoms in the small cavities at **C3**. This behavior corresponds to a conventional substitution alloy (Fig. 8a). Finally, at $x = 0.5$, all Na atoms at **C3** are substituted, so that **C3** is half occupied by Li. Now, for $0.5 < x \leq 1$, the Li atoms fill up the remaining vacant **C3** positions, while Na atoms at **C1** evanish (Fig. 7b). This exchange mechanism is unconventional as it represents an intermediate between an interstitial and a substitution alloy. The Li atoms occupy interstitial positions but simultaneously replace Na atoms located at other positions (Fig. 8b). At $x = 1$, **C3** is completely filled by Li and **C1** is completely emptied. Deviations of the experimental results from the substitution model only occur for low Na occupancies and Li positions, as expected. Seemingly, the occupancy of the narrow **C3** cavities has a stronger impact on the cell volume than the occupancy of **C1**, sharing the large channels with **C2**. This is also reflected in the distortion of the six-membered ring planes (Fig. 4). While the lattice parameters a and b in $NaLiGa_7$ nearly exhibit the ideal hexagonal ratio (Table 1), the value deviates significantly in Na_2Ga_7. When the Na atoms in the small **C3** cavities are replaced by Li in the range of $0 \leq x \leq 0.5$, the ratio approaches the hexagonal value (Fig. 7c). Conversely, the occupation of the **C1** position by Na in the range of $0.8 \leq x \leq 1$ has no influence on the axis ratio.

The proposed substitution mechanism finds further support in the interatomic distances of the Na atoms at **C2**, located within the channels of the Ga framework. In $NaLiGa_7$, the Na atoms at **C2** show uniform distances from each other (Fig. 4d). Conversely, in Na_2Ga_7, the channels are shared by Na
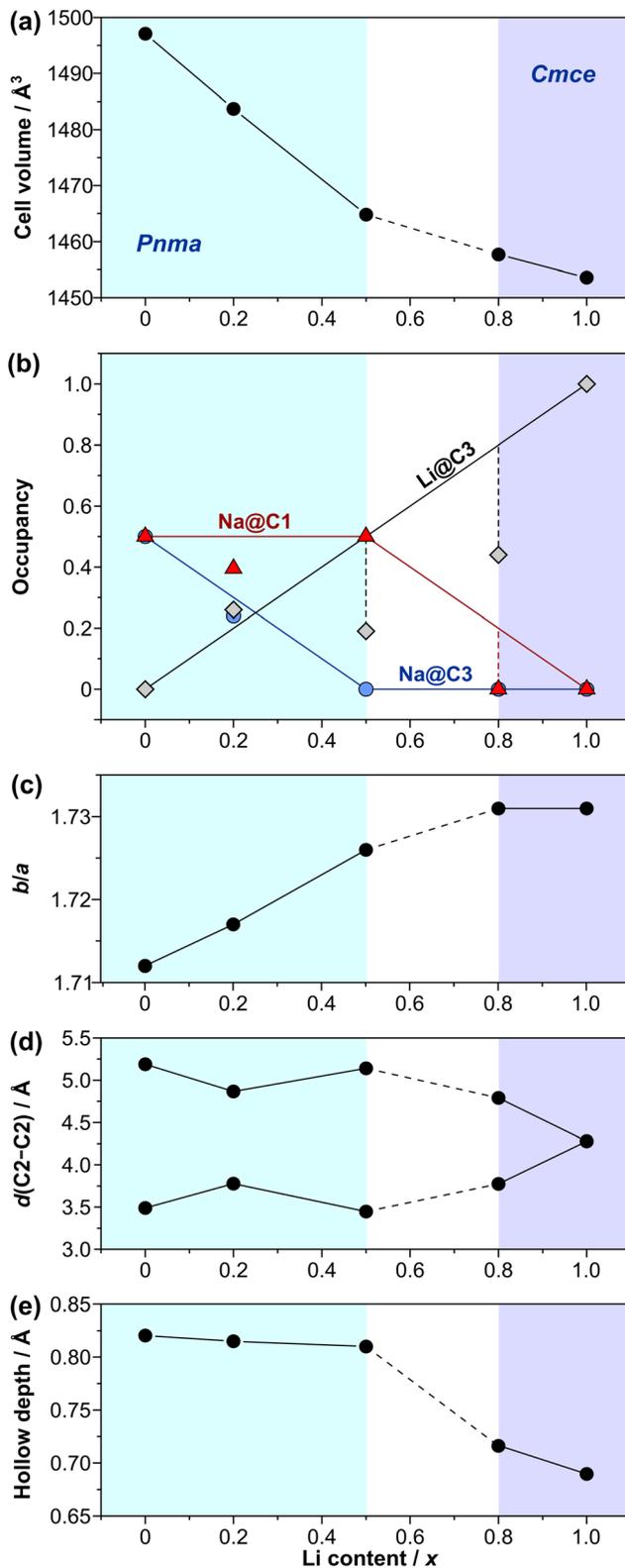
Fig. 7 (a) Cell volume of $Na_{2-x}Li_xGa_7$ ($x = 0, 0.2, 0.5, 0.8, 1$) against Li content. (b) Substitution model (lines) and refined occupancies (red triangles: Na at **C1**; blue circles: Na at **C3**; black circles: Li at **C3**). (c) b/a ratio of the hexagon planes. (d) Na–Na distances at position **C2**. (e) Depths of the hollow at **C1**. Shaded areas show the assumed homogeneity ranges. Error bars for all figures are smaller than the symbols used.
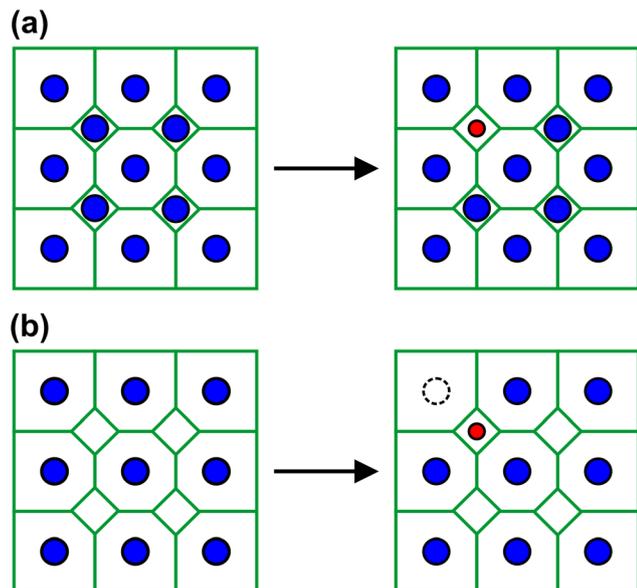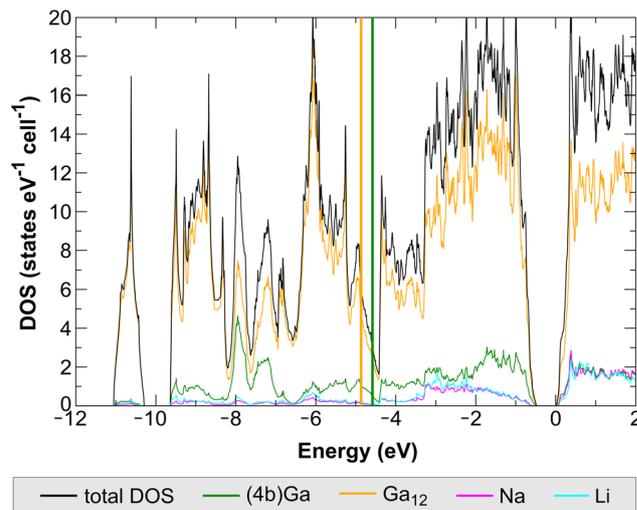
Fig. 8 (a) Scheme of a substitution alloy. (b) The unconventional intermediate of an interstitial and a substitution alloy. Green lines symbolize the Ga framework, blue spheres Na and red spheres Li.

Fig. 9 Computed electronic density of states (total DOS) for $NaLiGa_7$ and local DOS projections of the $[(4b)Ga]^-$ species, the summed $[(12b)Ga_{12}]^{2-}$ cluster species, and the cationic species. Thick vertical lines indicate energetical center of gravities of the $[(4b)Ga]^-$ local DOS (green) and the corresponding sum for $[(12b)Ga_{12}]^{2-}$ species (orange).

atoms at **C2** and **C1**, resulting in mutual repulsion that leads the Na atoms at **C2** to form dumbbells (Fig. 4c). Therefore, the refined distance between **C2** atoms is a signature of the Na occupancy at position **C1**. Starting from Na_2Ga_7, the experimentally determined Na–Na distances at **C2** remain constant for $0 \leq x \leq 0.5$, indicating the occupation of position **C1** (Fig. 7d). For $x > 0.5$ the distances converge to a common value, signifying vacancies at **C1**. Moreover, the occupancy of **C1** by Na affects the adjacent Ga atoms. The Na atoms at **C1** are situated in a hollow formed by three Ga six-membered rings (Fig. 2b). As **C1** becomes vacant, the depth of the hollows decreases (Fig. 7e and Fig. S6†). The decrease clearly starts for $x > 0.5$, in agreement with the proposed substitution model.

The X-ray results in this work suggest that the two boundary phases, Na_2Ga_7 and $Na_1Li_1Ga_7$, each have a homogeneity range. However, the two-phase region between both solid solutions was not detected in this study. In general, the ternary phase diagram Na–Li–Ga is unknown so far. A key challenge in determining the phase equilibria in future work will be the metallographic treatment of the air and moisture sensitive samples.

Electronic density of states

The computed electronic density of states (DOS) for $NaLiGa_7$ reveals a band gap of 0.47 eV (Fig. 9). This result is in line with the expectation of an electronically balanced composition for $[(12b)Ga_{12}]^{2-}$ icosahedral *closo* clusters and $[(4b)Ga]^-$ atoms. The Ga contributions are classified into two groups: (i) sum of the partial DOS of the Ga atoms forming the icosahedra Ga_{12}; (ii) DOS contributions of the 4-bonded Ga. These two chemically different Ga species are expected to be distinguishable in their local DOS projections.

The $[(4b)Ga]^-$ species do not significantly participate in the lowest-lying cluster orbital below −10 eV, containing 2 e⁻ per Ga_{12} cluster, and the computed energetical center of gravity of the (5 + 1)-fold coordinated cluster Ga species lies energetically lower than the one for the 4-fold coordinated one (Fig. 9). All these results are in good agreement with the results previously found for Na_2Ga_7 (calculated band gap = 0.29 eV).[5] As the DOS reveals (Fig. 9), there is no fundamental difference in the contribution of Na and Li atoms to the electronic structure of $NaLiGa_7$. We attribute the differences in the band gap between both compounds mainly to the larger distortions of the Ga icosahedra in Na_2Ga_7 (Fig. 6). The significant variation in the nearest neighbor distances is expected to result in a smaller intra-icosahedral band gap, which is of the bonding-antibonding type.[26,27]

Physical properties

The magnetization $M(T)$ of the sample of $NaLiGa_7$ was measured in the temperature range from $T = 1.8$ K to 400 K in magnetic fields $\mu_0 H = 0.002$ T, 0.1 T, 3.5 T and 7 T. The magnetic moment of the sample holder was subtracted from the measured data and the magnetic susceptibility $\chi = M/H$ was calculated. The magnetic susceptibility $\chi(T)$ is temperature-independent and diamagnetic (Fig. S7†) with value $\chi = -1.70 \times 10^{-4}$ emu mol⁻¹ per formula unit, agreeing within 1% with the calculated value (-1.59×10^{-4} emu mol⁻¹) from diamagnetic increments for Na^+, Li^+ and elemental Ga.[28] The superconductivity observed below $T \approx 8$ K can be attributed to the presence of elemental Ga impurities since the Meissner fraction of the signal is low ($\approx 0.09\%$). From the reported data, the allotropes β-, γ- and δ-Ga show superconducting transitions at 5.9 K–6.2 K, 6.9 K–7.6 K and 7.85 K, respectively.[29] The resistivity measurements on $Na_{2-x}Li_xGa_7$ were challenging because of

the tendency to form elemental Ga segregation on the surface of the sample during the measurements caused by oxidation.

Conclusions

The pseudo-binary system $Na_{2-x}Li_xGa_7$ is terminated by the compositions Na_2Ga_7 and $Na_1Li_1Ga_7$. Both phases show a homogeneity range with different substitution mechanisms. The crystal structure of $Na_1Li_1Ga_7$ belongs to the $MgB_{12}Si_2$ structure family, characterized by a framework of *closo* Ga_{12} icosahedra and 4-bonded Ga atoms. Within the Ga framework, the alkali metal atoms occupy distinct channels and cavities. For $Na_1Li_1Ga_7$, the arrangement of cations is fully ordered, representing a new variant within the $MgB_{12}Si_2$ structure family. $Na_1Li_1Ga_7$ was prepared by either annealing the elements or by the quantitative metathesis reaction of Na_2Ga_7 with LiCl. Considering the electron balance $[Na^+]_8[Li^+]_8[(12b)$ $Ga_{12}^{2-}]_4[(4b)Ga^-]_8$, the compound can be classified as a Zintl–Wade phase. The balance is consistent with the diamagnetic susceptibility and an electronic band gap, calculated to be 0.47 eV.

Author contributions

Chia-Chi Yu: investigation, formal analysis, conceptualization, methodology, writing – original draft; Yurii Prots: investigation, conceptualization, writing – review & editing; Alim Ormeci: investigation, writing – review & editing; Mitja Krnel: investigation, writing – review & editing; Marcus Schmidt: investigation; Lev Akselrud: formal analysis; Frank R. Wagner: formal analysis, writing – review & editing; Yuri Grin: formal analysis, conceptualization, methodology, writing – review & editing; Michael Baitinger: formal analysis, conceptualization, methodology, writing – original draft.

Conflicts of interest

There are no conflicts to declare.

Acknowledgements

References

1 *The Physics and Chemistry of Inorganic Clathrates*, ed. G. S. Nolas, Springer Series in Materials Science, 2014.

2 B. Albert and H. Hillebrecht, *Angew. Chem., Int. Ed.*, 2009, **48**, 8640.

3 L. Pauling and S. Weinbaum, *Z. Kristallogr.*, 1934, **87**, 181.

4 C. Zheng and R. Hoffmann, *Z. Naturforsch., B: J. Chem. Sci.*, 1986, **41**, 292.

5 C.-C. Yu, A. Ormeci, I. Veremchuk, X.-J. Feng, Yu. Prots, M. Krnel, P. Koželj, M. Schmidt, U. Burkhardt, B. Böhme, L. Akselrud, M. Baitinger and Yu. Grin, *Inorg. Chem.*, 2023, **62**, 9054.

6 T. Ludwig and H. Hillebrecht, *J. Solid State Chem.*, 2006, **79**, 1623.

7 N. Vojteer, M. Schroeder, C. Röhr and H. Hillebrecht, *Chem. – Eur. J.*, 2008, **14**, 7331.

8 L. Akselrud and Yu. Grin, *J. Appl. Crystallogr.*, 2014, **47**, 803.

9 *Diamond V4.6.8, Crystal Impact*, 2022.

10 K. Koepernik and H. Eschrig, *Phys. Rev. B: Condens. Matter Mater. Phys.*, 1999, **59**, 1743.

11 J. P. Perdew and J. Wang, *Phys. Rev. B: Condens. Matter Mater. Phys.*, 1922, **45**, 13244.

12 C. Belin and R.-G. Ling, *J. Solid State Chem.*, 1982, **45**, 290.

13 J. Sappl and C. Hoch, *Inorg. Chem.*, 2020, **59**, 6566.

14 P. W. Atkins, T. L. Overton, J. P. Rourke, M. T. Weller and F. A. Armstrong, *Shriver and Atkins' Inorganic Chemistry*, W. H. Freeman and Company, New York, 5th edn, 2010.

15 W. T. Barrett and W. E. Wallace, *J. Am. Chem. Soc.*, 1954, **76**, 366.

16 G. Bruzzone, *Acta Crystallogr., Sect. B: Struct. Crystallogr. Cryst. Chem.*, 1969, **25**, 1206.

17 U. Frank-Cordier, G. Cordier and H. Schäfer, *Z. Naturforsch., B: J. Chem. Sci.*, 1982, **37**, 119.

18 K. Ghosh, A. Ovchinnikov, M. Baitinger, M. Krnel, U. Burkhardt, Yu. Grin and S. Bobev, *Dalton Trans.*, 2023, **52**, 10310.

19 K. Ghosh and S. Bobev, *Chem. – Eur. J.*, 2023, **29**, e20230238.

20 M. Kotsch, Yu. Prots, A. Ormeci, M. Bobnar, F. R. Wagner, A. Senyshyn and Yu. Grin, *Eur. J. Inorg. Chem.*, 2020, **29**, 2842.

21 K. Wade, *J. Chem. Soc. D*, 1971, **15**, 792.

22 K. Wade, *Adv. Inorg. Chem. Radiochem.*, 1976, **18**, 1.

23 H. G. von Schnering, *Angew. Chem., Int. Ed. Engl.*, 1981, **20**, 33.

24 Yu. Grin, U. Schwarz and W. Steurer, *Crystal Structure and Chemical Bonding. In Alloy Physics: A Comprehensive Reference*, ed. W. Pfeiler, Wiley-VCH, Weinheim, 2007; pp. 19.

25 T. F. Fässler, *Zintl Phases: Principles and Recent Developments*, Springer, Berlin-Heidelberg, 2011.

26 H. C. Longuet-Higgins and M. De V. Roberts, *Proc. R. Soc. London, Ser. A*, 1955, **230**, 110.

27 K. Wade, *Electron Deficient Compounds*, Springer, New York, 1971.

28 *Diamagnetic Susceptibility and Anisotropy of Inorganic and Organometallic Compounds*, ed. R. R. Gupta, Springer, Berlin-Heidelberg, 2007.

29 Y. Quan, P. J. Hirschfeld and R. G. Hennig, *Phys. Rev. B*, 2021, **104**, 075117.